RSC Advances




ROYAL SOCIETY OF CHEMISTRY

www.rsc.org/advances

Journal Name

ARTICLE

# Synthesis and highly enhanced acetylene sensing properties of Au nanoparticle-decorated hexagonal ZnO nanorings†

Received 00th January 20xx,
Accepted 00th January 20xx

DOI: 10.1039/x0xx00000x

www.rsc.org/

Chao Li,[a, c] Ying Lin,[a, c] Feng Li,[a, c] Linghui Zhu,[a, c] Fanxu Meng,*[b], Dongming Sun,[a] Jingran Zhou,*[a], Shengping Ruan*[c]

Hexagonal ZnO nanorings were synthesized by a one-step hydrothermal method and Au nanoparticles were decorated on the surface of ZnO nanorings through a facile deposition process. The as-prepared ZnO nanorings showed the well-defined hexagonal shape with a width of 0.75 μm ~ 1.4 μm, a thickness of 0.17 μm ~ 0.33 μm and a hollow size of 0.2 μm ~ 1 μm. For the Au nanoparticle-decorated hexagonal ZnO nanorings (Au-ZnO nanorings), Au nanoparticles with a size of 3 nm ~ 10 nm distributed discretely on the surface of ZnO nanorings. The acetylene sensing performance of the ZnO nanorings and Au-ZnO nanorings were tested. The results indicated that the Au-ZnO nanorings showed a higher response (28 to 100 ppm acetylene), lower operating temperature (255 °C), faster response/recovery speed (less than 9 s and 5 s, respectively), and lower detectable acetylene minimum concentration (about 1 ppm). In addition, the machenism about the enhanced acetylene-sensing performance of the Au-ZnO nanorings were discussed.

## Introduction

Zinc oxide (ZnO), a n-type metal oxide semiconductor with a wide direct band gap (3.37 eV), high exciton binding energy (60 meV) and piezoelectricity at room temperature,[1-3] has been attracted great interest in catalysis,[4, 5] photodetection,[6, 7] solar cell,[8, 9] pressure sensor[10, 11] and lithium ion battery[12, 13] etc. In gas-sensing field, ZnO has been recognized as an excellent gas-sensing material for the detection of combustible and toxic gas, and volatile organic compounds including hydrogen,[14] carbon monoxide,[15] nitric oxide,[16] ethanol,[17] acetone,[18, 19] and formaldehyde[20] etc. due to its biocompatibility, non-toxicity, stability, low-cost, ease of large scale fabrication and superior sensing properties.

Recent years, nano- and micro-scale ZnO with various morphologies such as nanopaticle,[17] nanorod,[15] nanowire,[21] nanofiber,[22] nanoplate[23] and nanosheet,[24] etc. have been synthesized. Compared with these morphologies, nanoring shows a specific two-dimensional (2D) structure that can be regarded as one-dimensional (1D) nanostructure bending into the 2D nanostructure in a plain. And such a structure make nanoring has the advantages of 1D, 2D and hollow nanostructures including slight agglomeration, high specific surface area and excellent porosity etc., which are beneficial to accelerate gas diffusion and improve gas-sensing performance for the gas-sensing materials.

For many gas sensors, the response is determined by the efficiency of catalytic reactions with detected gas participation, taking place at the surface of gas-sensing material.[25] However, in practice, the widely used gas-sensing metal oxides exhibit the poor catalytic active and sensitivity to detected gas. Latest years, it has been proved that metallic catalysts such as Ag,[26] Au,[27-29] Pd,[30] and Pt[31] nanoparticles loaded onto the surfaces of the metal oxide supports serve as sensitizers or promoters, dramatically improving the sensitivity, response and recovery time, and operating temperature. Moreover, the catalytic active of noble metal is sharply enhanced with the decrease in its size and noble metal nanoparticles with small size and discrete distribution have the greater advantage in gas-sensing field.[32]

At present, many gas sensors with high properties have been obtained in detecting ethanol, acetone, nitric oxide, xylene and carbon monoxide etc. However, the researches on the acetylene ($C_2H_2$) are not enough. Acetylene is the most effective and versatile fuel gas, enabling manual applications in welding, cutting, straightening and other localized heating process. Moreover, acetylene is a kind of colourless and odorless gas which is not easy to detect in the air and highly combustible and explosive. Therefore, great efforts are required to fabricate practical acetylene sensor.

In this work, ZnO nanorings with the well-defined hexagonal shape were synthesized by a one-step hydrothermal method. Then Au nanoparticles with a size of 3 nm ~ 10 nm were

[a] State Key Laboratory on Integrated Optoelectronics, Jilin University, Changchun 130012, P. R. China.
E-mail: zhoujr@jlu.edu.cn (J. Zhou)
[b] Jilin Institute of Chemical Technology, Jilin City, 132022, PR China.
E-mail: E-mail: fxmengjlu@gmail.com (F. Meng)
[c] College of Electronic Science and Engineering, Jilin University, Changchun 130012, PR China.
E-mail: Ruansp@jlu.edu.cn (S. Ruan)
† Electronic Supplementary Information (ESI) available. See DOI: 10.1039/x0xx00000x

discretely decorated on the surface of ZnO nanorings through a facile deposition process. The acetylene sensing performance of the ZnO nanorings and Au-ZnO nanorings were tested and the results indicated that the Au-ZnO nanorings showed greatly improvement including the higher response, lower operating temperature, faster response/recovery speed and lower detectable acetylene minimum concentration. In addition, the mechanism about the enhanced acetylene-sensing performance of the Au-ZnO nanorings was discussed.

## Experimental section

### Materials

All the starting agents were used without purification. Zinc nicetate hexahydrate ($Zn(NO_3)_2{\cdot}6H_2O$) and hexamethylenetetramine ($C_6H_{12}N_4$, HMTA) were purchased from the Xilong Chemical Co., Ltd. Polyvinyl alcohol 1788 (PVA-1788) and polyvinylpyrrolidone (PVP, K 88-96) were purchased from Aladdin chemistry Co., Ltd.

### Preparation of hexagonal ZnO nanorings

The typical preparation of hexagonal ZnO nanorings are described as follows: 0.297 g $Zn(NO_3)_2{\cdot}6H_2O$, 0.28 g HMTA and 0.4 g PVP were successively dissolved in 20 mL deionized water under stirring at room temperature. When the PVP completely dissolved, a certain amount of PVA-1788 was added into above solution under stirring. After the PVA-1788 was dissolved completely, the resulting solution was gradually heated to 90 °C through the water bath and kept for 10 min under stirring. Then the resulting white suspension was transferred into a 30 mL Teflon-lined stainless steel autoclave for hydrothermal treatment at 90 °C for 6 h. After cooling down to room temperature, the products were rinsed with hot deionized water several times followed by drying in air at 60 °C overnight. The formation mechanism of ZnO nanorings was presented in Fig. S1.†

### Preparation of Au nanoparticle-decorated ZnO nanorings

Au nanoparticles were decorated on the surface of ZnO nanorings according to the procedure in the literature.[33] In a typical synthesis, 0.0163 g (0.20 mmol) as-prepared ZnO nanorings were dispersed in 11.50 mL deionized water under ultrasonic treatment, then 7.50 mL $HAuCl_4$ (0.02 M) aqueous solution and 1.00 mL $NH_3{\cdot}H_2O$ were added in order to the suspension. After stirring for about 3 h, the precipitate was collected by centrifugation and washed with deionized water several times. Finally, the Au nanoparticle-decorated ZnO nanorings (denoted as Au- ZnO nanorings) were obtained by annealing the precursor at 350 °C for 1 h in a muffle furnace. The mechanism of Au decoration was presented in Fig. S1.†

### Characterization

The sample were characterized by powder X-ray diffractometer (XRD, Shimadzu XRD-6000 with Cu Kα radiation, λ = 0.154178 nm), scanning electron microscopy (SEM, JSM6700F), energy-dispersive X-ray diffraction (EDX), selected area electron diffraction (SAED) and transmission electron microscopy (TEM, FEI Tecnai F20).

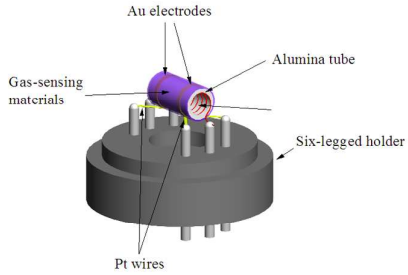


**Fig. 1.** Sketch of gas sensor.

### Gas sensor fabrication and test

The fabricating process of sensors in brief: The as-prepared ZnO were mixed with deionized water in a weight ratio of 100: 25 to form a paste. The paste was coated onto a ceramic tube on which a pair of gold electrodes was previously printed, and then a Ni-Cr heating wire was inserted in the tube to form a side-heated gas sensor. The fabricated sensor is shown in Fig. 1.

Gas sensing properties were measured by a CGS-8 (Chemical gas sensor-8) intelligent gas sensing analysis system (Beijing Elite Tech Co. Ltd., China). The gas response was defined as $S = R_a/R_g$, where the $R_g$ and $R_a$ are the resistance values of sensors in the presence and absence of the target gas, respectively. The time taken by the sensor to achieve 90% of the total resistance change was defined as the response time in the case of adsorption or the recovery time in the case of desorption. The detectable minimum is defined as the concentration makes the response of sensor reach to 3.

## Results and discussion

The crystal structures of ZnO nanorings and Au-ZnO nanorings

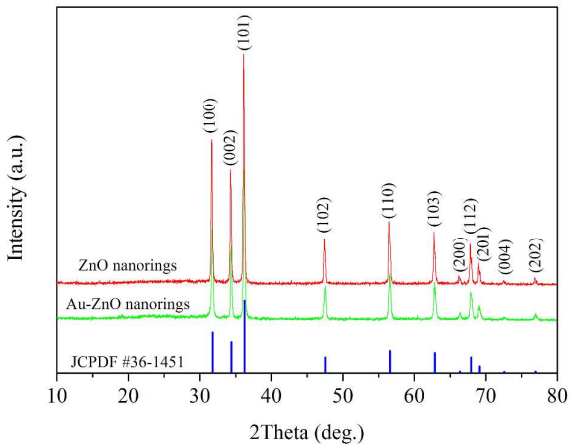


**Fig. 2.** XRD patterns of ZnO and Au-ZnO nanorings.

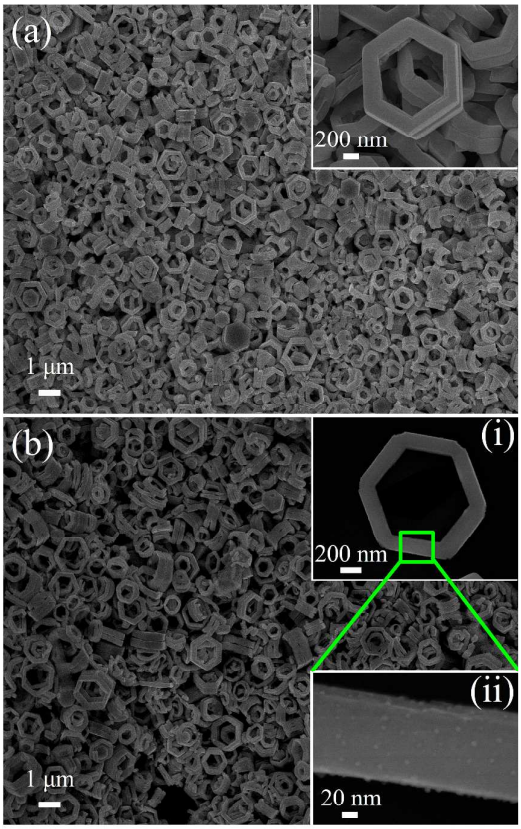


**Fig. 3.** Low- and high-magnification SEM images of (a) the ZnO nanorings and (b) Au-ZnO nanorigns.

were examined by XRD, as shown in Fig. 1. It can be seen that the diffraction patterns of ZnO nanorings, at 2θ = 31.8 °, 34.4 °, 36.8 °, 47.5 °, 56.6 °, 62.9 °, 66.4 °, 68.0 °, 69.1 °, 71.6 ° and 77.0 ° correspond to (100), (002), (101), (102), (110), (103), (200), (112), (201), (004) and (202) characteristic peaks of wurtzite ZnO (JCPDS: 36-1451), respectively. For Au-ZnO nanorings, all the diffraction peaks belong to ZnO and no diffraction peak corresponding to Au can be found which may be attributed to the discrete distribution and small size of Au nanoparticles.[26]

The SEM images of the ZnO nanorings and Au-ZnO nanorings are shown in Fig. 3(a) and (b). From Fig. 3(a), it can be seen that the ZnO nanorings show a hexagonal ring-like morphology with a width of 0.75 μm ~ 1.4 μm, a thickness of 0.17 μm ~ 0.33 μm and a hollow size of 0.2 μm ~ 1 μm. After Au nanoparticle-decoration process, Au-ZnO nanorings kept the original morphology of hexagonal ZnO nanorings. From the high magnification SEM images of Au-ZnO nanorings in inserts (i) and (ii), it can be seen that Au nanoparticles with a size range from 3 nm to 10 nm discretely distributed on the surface of ZnO nanorings. Such a small size can make Au nanoparticles show an excellent catalytic activity and thus enhance sensing properties of ZnO nanorings. In addition, the films composed by ZnO and Au-ZnO nanorings are both porous which facilitate the diffusion and distribution of surrounding gas phase to the

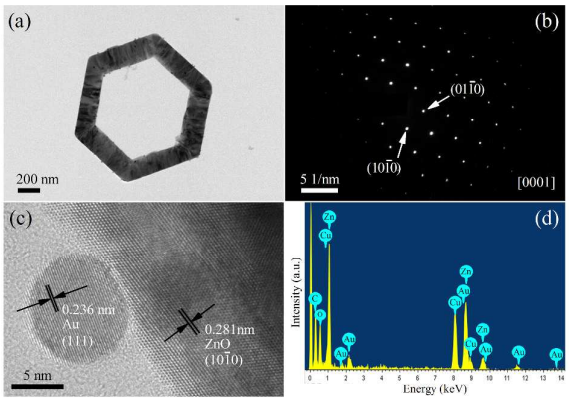


**Fig. 4.** (a) The low-magnification TEM image of single Au-ZnO nanoring; (b) The corresponding SAED pattern; (c) the high-magnification TEM image; (d) EDX spectra of Au-ZnO nanorings

surface of the internal films, which will increase the reaction sites and contribute to improving the gas sensing properties greatly.

In order to obtain more details, transmission electron microscopy TEM, selected area electron diffraction (SAED) and energy-dispersive X-ray diffraction (EDX) were employed to analyze the Au-ZnO nanorings. Fig. 4(a) shows a low-magnification TEM image of single Au-ZnO nanoring and a clear hexagonal ring-like outline can be observed. In addition, it also shows that Au nanoparticles attaching to the surface of the ZnO nanoring are just next to the outline. The SAED pattern shown in Fig. 4(b) can be indexed to the [0001] zone axis of single-crystal hexagonal ZnO nanoring, and this implies that the as-prepared ZnO nanorings are single-crystalline and the single Au-ZnO nanoring shown in Fig. 4(a) is viewed along the [0001] direction. In order to observe the microstructure of the Au-ZnO nanorings, high-magnification TEM (HRTEM) image is shown in Fig. 4(c). In the HRTEM image, the interplanar distance of 0.281 nm is close to the d spacings of the

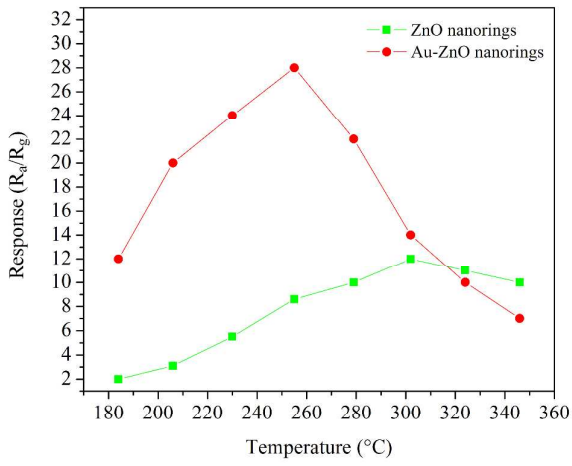


**Fig. 5.** Response of ZnO and Au-ZnO nanorings to 100 ppm acetylene as a function of the operating temperature.

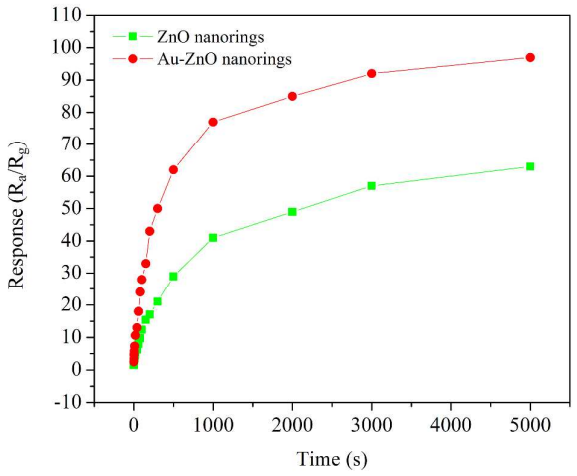


**Fig. 6.** Curves of sensors' responses versus acetylene concentrations at their optimum operating temperature.

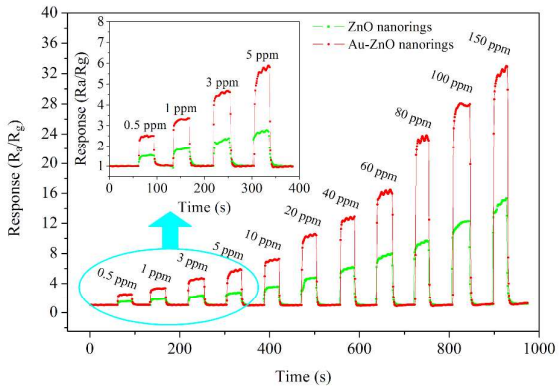


**Fig. 7.** Transient response of the ZnO and Au-ZnO nanorings

(10$\bar{1}$0) planes of the hexagonal structured ZnO nanoring. In addition, as shown in Fig. 4(c), the interplanar distance of 0.238 nm is close to the d spacings of the (111) planes of Au, and the size of the Au nanoparticle is about 10 nm which is in accord with the result of SEM. The corresponding EDX spectrum of the Au-ZnO nanoring are shown in Fig. 4(d). As can be seen, the EDX peaks around 1.03 keV, 8.64 keV and 9.53 keV can be indexed to Zn element, and the EDX peaks around 0.52 keV can be indexed to O element. What's more, the obvious EDX peaks of Au element are found around 2.10 keV, 9.71 keV and 11.58 keV certifying the presence of Au nanoparticles and the Au to Zn atomic ratio is about 6.6:100.

In order to find the optimum operating temperature of the sensors based on the hexagonal ZnO and Au-ZnO nanorings, their responses to 100 ppm acetylene at different operating temperatures (from 205 to 350 °C) were collected. As shown in Fig. 5, the response of sensors to acetylene increases with the augment of operating temperatures and attains the maximum values at a certain temperature, followed by a decrease. It can be seen that Au-ZnO nanorings obtain the maximum response 28 at 255°C which is much higher than 12 at 302 °C for ZnO nanorings which indicates Au nanoparticles contribute to the decrease in the operating temperature and increase in response to acetylene. So, 255 °C and 302 °C are designed as the optimal operating temperatures of Au-ZnO and ZnO nanorings respectively and the following acetylene-sensing performance is tested at their optimal operating temperatures.

The responses of the ZnO and Au-ZnO nanorings to different concentrations of acetylene are shown in Fig. 6. It can be easily found that the responses increase rapidly with increasing of the acetylene concentration, then gradually slow down and trend to saturation after the concentration beyond 1000 ppm. What's more, Au-ZnO nanorings had a higher response than that of ZnO nanorings at each acetylene concentration.

As for gas sensing applications, rapid response and recovery is of great importance to real-time monitor. To investigate the response-recovery behaviors of the hexagonal ZnO and Au-ZnO nanorings, the sensor was sequentially exposed to 0.5, 1, 3, 5, 10, 20, 40, 60, 80, 100 and 150 ppm acetylene, respectively. As shown in Fig. 7, when sensors exposed to acetylene the response increases rapidly and when subjected to air the sensor' recovery to the initial state is also rapid. Compared with ZnO nanorings, Au-ZnO nanorings show the higher response, faster response/recovery speed and lower detectable minimum to acetylene. Au-ZnO nanorings shorten the response time from 6 s ~ 15 s to 3 s ~ 11 s and the recovery time from 5 s ~ 9 s to 2 s ~ 5 s. And Au-ZnO nanorings reduce the detectable minimum from below 10 ppm (between 5 ppm

Table 1. Comparisons of acetylene sensors within this work and with some reported literatures.

| Materials | | Operating temperature | response | Response/recovery time | Detectable limit |
|---|---|---|---|---|---|
| $Sm_2O_3$-doped $SnO_2$[34] | | 180 °C | 63.8 | 12 s / 30 s | > 10 ppm |
| $Cd_2Sb_2O_{6.8}$[35] | | 360 °C | About 9 (100 ppm) | ---[a] | --- |
| 2 at.% Pt/ZnO[36] | | 300 °C | 165 (500 ppm) | 11 s / --- | 50 ppm |
| Ag-loaded hierarchical ZnO nanostructure-reduced graphene oxide[37] | | 200 °C | 13 (100 ppm) | About 45 s / 115 s (100 ppm) | < 10 ppm |
| ZnO/reduced graphene oxide[38] | | 250 °C | 18.2 (100 ppm) | 31 s / 9 s (100 ppm) | 10 ppm |
| This work | ZnO nanorings | 302 °C | 12 (100 ppm) | 8 s / 5 s (100 ppm) | < 10 ppm |
| | Au-ZnO nanorings | 255 °C | 28 (100 ppm) | 4 s / 3 s (100 ppm) | < 1 ppm |

[a] The short line presents the corresponding data is not spelled out in the literature.

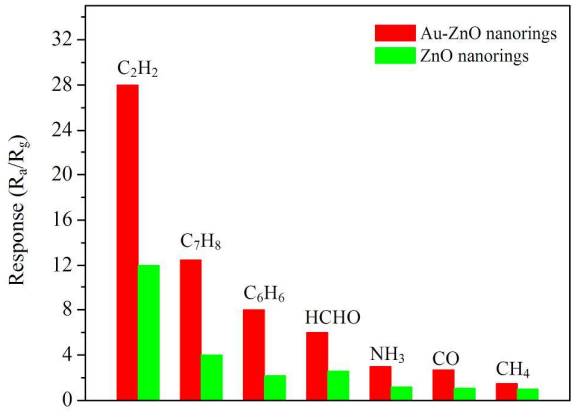


**Fig. 8** Selectivity of the hexagonal ZnO nanorings and Au-ZnO nanorings toward acetylene ($C_2H_2$), toluene ($C_7H_8$), benzene ($C_6H_6$), formaldehyde (HCHO), ammonium ($NH_3$), carbon monoxide (CO) and methane ($CH_4$).

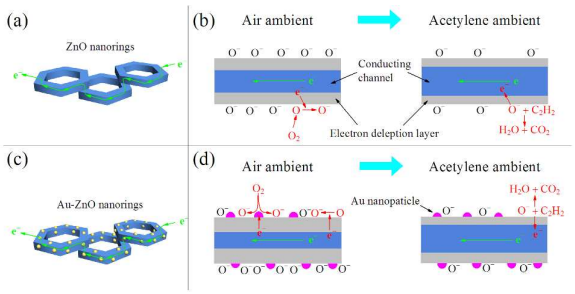


**Fig. 9.** (a) and (c) The electronic transmission path within and between ZnO and Au-ZnO nanoring(s), respectively; (b) and (d) acetylene-sensing mechanism of ZnO and Au-ZnO nanorings, respectively.

and 10 ppm, and the corresponding responses are 2.8 and 3.6, respectively) to below 1 ppm (between 0.5 ppm and 1 ppm, and the corresponding responses are 2.5 and 3.3, respectively)). To certify the statistical significance, the sensors were measured for 5 times in 0.5 ppm and 1 ppm acetylene ambience, respectively, as shown in Fig. S2.† In addition, the repeatability of the ZnO and Au-ZnO nanorings to 100 ppm acetylene were shown in Fig. S3.† These results indicate Au-ZnO nanorings are more advantageous than ZnO nanorings for acetylene detection.

Comparisons among ZnO nanorings, Au-ZnO nanorings and other reported acetylene-sensing materials are displayed in Table 1. As can be seen, the Au-ZnO nanorings have an advantage in detecting acetylene due to the high response, low detectable limit, fast response/recovery speed as well as low operating temperature.

The gas sensing selectivity is another important parameter to evaluate the sensing ability of oxide semiconductor materials. Fig. 8 shows the cross-sensitivities of the hexagonal ZnO nanorings and Au-ZnO nanorings to 100 ppm various gases including acetylene ($C_2H_2$), toluene ($C_7H_8$), benzene ($C_6H_6$), formaldehyde (HCHO), ammonium ($NH_3$), carbon monoxide (CO) and methane ($CH_4$). It is clear that both the hexagonal ZnO nanorings and Au-ZnO nanorings exhibit the largest responses towards acetylene among the tested gases and show good selectivity to acetylene.

The acetylene sensing mechanisms of the ZnO nanorings and Au nanoparticle-decorated ZnO nanorings can be explained as follows and illustrate in Fig. 9(a)-(d). Fig. 9(a) illustrates the electronic transmission path within and between ZnO nanoring(s). Fig. 9(b) shows the vertical section of an edge of ZnO nanoring. Response of semiconducting metal oxides is based on the reactions between target gas molecule and the oxygen species on the surface of oxides.[39, 40] ZnO is an n-type semiconductor and its resistance is mainly determined by the conduction band electrons. As shown in Fig. 9(b), when the hexagonal ZnO nanorings are surrounded by air, oxygen molecules can be adsorbed on their surface to generate chemisorbed oxygen species by capturing electrons from the conduction band of ZnO. As a result, a wide electron depletion layer generates next to the surface of ZnO nanorings and it narrows the electronic conducting channel, which can lead to an increase in ZnO nanorings' resistance. When the sensor is exposed to acetylene, acetylene molecules can react with the chemisorbed oxygen species ($O^-$ is believed to be dominant at sensor's operating temperature[41, 42]) and release the trapped electron back to the conduction band, which will diminish the depletion layer, widen the electronic conducting channel and result in the decrease in ZnO nanorings' resistance. When exposed to air again, chemisorbed oxygen species will increase and ZnO nanorings' resistance will recover to high value. In a word, ZnO nanorings will response to ambience change through the decrease (from air to acetylene ambience) or increase (from acetylene to air ambience) in resistance. The reaction between chemisorbed oxygen species and acetylene can be simply described as:

$$C_2H_2 + 5\ O^- = H_2O + 2\ CO_2 + 5\ e^- \qquad (1)$$

The highly enhanced acetylene-sensing properties of Au-ZnO nanorings can be mainly attributed to catalytic oxidation of acetylene induced by Au nanoparticles. It has been reported that Au nanoparticles supported on metal oxide semiconductors showed the catalytic ability for acetylene oxidation. For Au-ZnO nanorings' case, the reaction between acetylene and $O^-$ spices is promoted, and as a result, a higher response, faster response/recovery speed and lower operating temperature are obtained. Fig. 9(c) illustrates the electronic transmission path within and between Au-ZnO nanoring(s) and Fig. 9(d) shows the vertical section of an edge of Au-ZnO nanoring. In addition, Au nanoparticles can effectively accelerate the transformation of $O_2$ to $O^-$ spices which will deepen electron depletion layer (as shown in Fig. 9(d)) and make Au-ZnO nanorings show a higher atmospheric resistance (as shown in Fig. S4, ESI†).[43, 44] Therefore, when Au-ZnO nanorings expose to acetylene, a larger resistance change i.e. higher response generates.

Moreover, the porous structure of the acetylene-sensing film composed by Au-ZnO nanorings is beneficial to gas

diffusion and provides more active sites for oxygen adsorption and the reaction between adsorbed oxygen species and acetylene, which also contributes to the high response and rapid response/recovery rate.

## Conclusions

In conclusion, hexagonal ZnO nanorings were synthesized by a one-step hydrothermal method and Au nanoparticles were decorated on the surface of ZnO nanorings through a facile deposition process. The as-prepared ZnO nanorings showed the well-defined hexagonal shape with a width of 0.75 μm ~ 1.4 μm, a thickness of 0.17 μm ~ 0.33 μm and a hollow size of 0.2 μm ~ 1 μm. For the Au nanoparticle-decorated ZnO nanorings (Au-ZnO nanorings), Au nanoparticles with a size of 3 nm ~ 10 nm distributed discretely on the surface of ZnO nanorings. The acetylene sensing performance of the ZnO nanorings and Au-ZnO nanorings were tested. The results indicated that the Au-ZnO nanorings showed a higher response (28 to 100 ppm acetylene), lower operating temperature (255 °C), faster response/recovery speed (less than 9 s and 5 s, respectively), and lower detectable acetylene minimum concentration (about 1 ppm).

## Acknowledgements

This work was supported by the National Natural Science Foundation of China (Grant Nos. 61274068 and 61404058), Project of Science and Technology Plan of Changchun City (Grant No. 14KG020) and Opened Fund of the State Key Laboratory on Integrated Optoelectronics (Grant No. IOSKL2013KF10).

## Notes and references

1 S. Aksoy, Y. Caglar, S. Ilican and M. Caglar, *J. Alloy Compd.*, 2012, **512**, 171-178.
2 R. Chen, B. Ling, X. W. Sun and H. D. Sun, *Adv. Mater.*, 2011, **23**, 2199-2204.
3 B. Kumar and S.-W. Kim, *Nano Energy*, 2012, **1**, 342-355.
4 T. T. Vu, L. del Río, T. Valdés-Solís and G. Marbán, *J. Hazard. Mater.*, 2013, 246, 126-134.
5 T. Xu, L. Zhang, H. Cheng and Y. Zhu, *Appl. Catal. B-Environ.*, 2011, **101**, 382-387.
6 W. Park, G. Jo, W.-K. Hong, J. Yoon, M. Choe, S. Lee, Y. Ji, G. Kim, Y. H. Kahng and K. Lee, *Nanotechnology*, 2011, **22**, 205204.
7 D. Gedamu, I. Paulowicz, S. Kaps, O. Lupan, S. Wille, G. Haidarschin, Y. K. Mishra and R. Adelung, *Adv. Mater.*, 2014, **26**, 1541-1550.
8 S. H. Ko, D. Lee, H. W. Kang, K. H. Nam, J. Y. Yeo, S. J. Hong, C. P. Grigoropoulos and H. J. Sung, *Nano letters*, 2011, **11**, 666-671.
9 K. A. Salman, K. Omar and Z. Hassan, *Solar Energy*, 2012, **86**, 541-547.
10 A. Wei, L. Pan and W. Huang, *Mater. Sci. Eng. B-Solid*, 2011, **176**, 1409-1421.
11 X. J. Zheng, X. Cao, J. Sun, B. Yuan, Q. Li, Z. Zhu and Y. Zhang, *Nanotechnology*, 2011, **22**, 435501.
12 X. Huang, X. Xia, Y. Yuan and F. Zhou, *Electrochimica Acta*, 2011, **56**, 4960-4965.
13 K. T. Park, F. Xia, S. W. Kim, S. B. Kim, T. Song, U. Paik and W. I. Park, *J. Phy. Chem. C*, 2013, **117**, 1037-1043.
14 D.-T. Phan and G.-S. Chung, *Sens. Actuators B-Chem.*, 2012, **161**, 341-348.
15 C.-M. Chang, M.-H. Hon and C. Leu, *RSC Advances*, 2012, **2**, 2469-2475.
16 M. Chen, Z. Wang, D. Han, F. Gu and G. Guo, *J. Phys. Chem. C*, 2011, **115**, 12763-12773.
17 T. T. Trinh, N. H. Tu, H. H. Le, K. Y. Ryu, K. B. Le, K. Pillai and J. Yi, *Sens. Actuators B-Chem.*, 2011, **152**, 73-81.
18 Y. Xiao, L. Lu, A. Zhang, Y. Zhang, L. Sun, L. Huo and F. Li, *ACS Appl. Mater. Inter.*, 2012, **4**, 3797-3804.
19 P. Song, Q. Wang and Z. Yang, *Materials Letters*, 2012, **86**, 168-170.
20 L. Zhang, J. Zhao, J. Zheng, L. Li and Z. Zhu, *Appl. Surf. Sci.*, 2011, **258**, 711-718.
21 M.-L. Zhang, F. Jin, M.-L. Zheng, J. Liu, Z.-S. Zhao and X.-M. Duan, *RSC Advances*, 2014, **4**, 10462-10466.
22 C. Lai, X. Wang, Y. Zhao, H. Fong and Z. Zhu, *RSC Advances*, 2013, **3**, 6640-6645.
23 Z. Jing and J. Zhan, *Adv. Mater.*, 2008, **20**, 4547-4551.
24 W. Guo, M. Fu, C. Zhai and Z. Wang, *Ceram. Int.*, 2014, **40**, 2295-2298.
25 C. Wang, L. Yin, L. Zhang, D. Xiang and R. Gao, *Sensors*, 2010, **10**, 2088-2106.
26 I.-S. Hwang, J.-K. Choi, H.-S. Woo, S.-J. Kim, S.-Y. Jung, T.-Y. Seong, I.-D. Kim and J.-H. Lee, *ACS Appl. Mater. Inter.*, 2011, **3**, 3140-3145.
27 L. Qian, K. Wang, Y. Li, H. Fang, Q. Lu and X. Ma, *Mater. Chem. Phys.*, 2006, **100**, 82-84.
28 X. Wang, S. Qiu, C. He, G. Lu, W. Liu and J. Liu, *RSC Advances*, 2013, **3**, 19002-19008.
29 Y.-S. Shim, H. G. Moon, D. H. Kim, L. Zhang, S.-J. Yoon, Y. S. Yoon, C.-Y. Kang and H. W. Jang, *RSC Advances*, 2013, **3**, 10452-10459.
30 S. Tian, X. Ding, D. Zeng, J. Wu, S. Zhang and C. Xie, *RSC* Advances, 2013, **3**, 11823-11831.
31 N. Tamaekong, C. Liewhiran, A. Wisitsoraat and S. Phanichphant, *Sensor. Actuat. B-Chem.,* 2011, **152**, 155-161.
32 A. K. Jaiswal, S. Singh, A. Singh, R. R. Yadav, P. Tandon and B. C. Yadav, *Mater. Chem. Phys.*, 2015, **154**, 16-21.
33 J. Zhang, X. Liu, S. Wu, M. Xu, X. Guo and S. Wang, *J.* Mater. *Chem.*, 2010, **20**, 6453.
34 Q. Qi, T. Zhang, X. Zheng, H. Fan, L. Liu, R. Wang and Y. Zeng, *Sens. Actuators B-Chem.*, 2008, **134**, 36-42.
35 Y. Liu, X. Liu and Y. Shen, *Sens. Actuators B-Chem.*, 1999, **55**, 9-13.
36 N. Tamaekong, C. Liewhiran, A. Wisitsoraat and S. Phanichphant, *Sens. Actuators B-Chem.*, 2011, **152**, 155-161.
37 A. I. Uddin, K.-W. Lee and G.-S. Chung, *Sens. Actuators B-Chem.,* 2015, **216**, 33-40.

38 A. I. Uddin and G.-S. Chung, *Sens. Actuators B-Chem.,* 2014, **205**, 338-344.
39 C.-M. Chang, M.-H. Hon and C. Leu, *RSC Advances*, 2012, **2**, 2469.
40 Q. Yu, C. Yu, J. Wang, F. Guo, S. Gao, S. Jiao, H. Li, X. Zhang, X. Wang and H. Gao, *RSC Advances*, 2013, **3**, 16619.
41 N. Barsan and U. Weimar, *J. Electroceram.*, 2001, **7**, 143.
42 Y.F. Sun, S.B. Liu, F.L. Meng, J.Y. Liu, Z. Jin, L.T. Kong and J.H. Liu, *Sensors*, 2012, **12**, 2610.
43 M. C. Kung, R. J. Davis and H. H. Kung, *J. Phys. Chem. C*, 2007, **111**, 11767.
44 P. Montmeat, J.-C. Marchand, R. Lalauze, J.-P. Viricelle, G. Tournier and C. Pijolat, *Sens. Actuators B-Chem.*, 2003, **95**, 83.